Original Article

The Role of Heparin Cofactor II in the Regulation of Insulin Sensitivity and Maintenance of Glucose Homeostasis in Humans and Mice

Kiyoe Kurahashi[1], Seika Inoue[2], Sumiko Yoshida[1], Yasumasa Ikeda[3], Kana Morimoto[4], Ryoko Uemoto[4], Kazue Ishikawa[1], Takeshi Kondo[1], Tomoyuki Yuasa[4], Itsuro Endo[1], Masato Miyake[5], Seiichi Oyadomari[5], Toshio Matsumoto[6], Masahiro Abe[1], Hiroshi Sakaue[2] and Ken-ichi Aihara[4]

[1]Department of Hematology, Endocrinology and Metabolism, Tokushima University Graduate School of Biomedical Sciences, Tokushima, Japan
[2]Department of Nutrition and Metabolism, Tokushima University Graduate School of Biomedical Sciences, Tokushima, Japan
[3]Department of Pharmacology, Tokushima University Graduate School of Biomedical Sciences, Tokushima, Japan
[4]Department of Community Medicine for Diabetes and Metabolic Disorders, Tokushima University Graduate School of Biomedical Sciences, Tokushima, Japan
[5]Division of Molecular Biology, Institute for Genome Research, Institute of Advanced Medical Sciences, Tokushima University, Tokushima, Japan
[6]Fujii Memorial Institute of Medical Sciences, Tokushima University, Tokushima, Japan

Aim: Accelerated thrombin action is associated with insulin resistance. It is known that upon activation by binding to dermatan sulfate proteoglycans, heparin cofactor II (HCII) inactivates thrombin in tissues. Because HCII may be involved in glucose metabolism, we investigated the relationship between plasma HCII activity and insulin resistance.

Methods and Results: In a clinical study, statistical analysis was performed to examine the relationships between plasma HCII activity, glycosylated hemoglobin (HbA1c), fasting plasma glucose (FPG), and homeostasis model assessment-insulin resistance (HOMA-IR) in elderly Japanese individuals with lifestyle-related diseases. Multiple regression analysis showed significant inverse relationships between plasma HCII activity and HbA1c ($p=0.014$), FPG ($p=0.007$), and HOMA-IR ($p=0.041$) in elderly Japanese subjects. In an animal study, $HCII^{+/+}$ mice and $HCII^{+/-}$ mice were fed with a normal diet or high-fat diet (HFD) until 25 weeks of age. HFD-fed $HCII^{+/-}$ mice exhibited larger adipocyte size, higher FPG level, hyperinsulinemia, compared to HFD-fed $HCII^{+/+}$ mice. In addition, HFD-fed $HCII^{+/-}$ mice exhibited augmented expression of monocyte chemoattractant protein-1 and tumor necrosis factor, and impaired phosphorylation of the serine/threonine kinase Akt and AMP-activated protein kinase in adipose tissue compared to HFD-fed $HCII^{+/+}$ mice. The expression of phosphoenolpyruvate carboxykinase and glucose-6-phosphatase was also enhanced in the hepatic tissues of HFD-fed $HCII^{+/-}$ mice.

Conclusions: The present studies provide evidence to support the idea that HCII plays an important role in the maintenance of glucose homeostasis by regulating insulin sensitivity in both humans and mice. Stimulators of HCII production may serve as novel therapeutic tools for the treatment of type 2 diabetes.

Key words: Glucose homeostasis, Heparin cofactor II, High-fat diet, Humans, Mice

Introduction

Previous clinical studies have provided considerable evidence for a relationship between obesity and thrombosis, citing the enhanced expression of pro-thrombotic molecules, including plasminogen activa-

1

tor inhibitor-1 and tissue factor, and increased platelet activation[1]. Additionally, it has been shown that the acceleration of thrombin action is associated with the development of insulin resistance, leading to metabolic syndrome and type 2 diabetes mellitus (T2DM)[2]. Thrombin activates platelets, vascular endothelial cells, vascular smooth muscle cells, macrophages, and fibroblasts via binding to their protease-activated receptors (PARs). PAR-1 activation by thrombin enhances procoagulation[3], chemoattraction[4], mitogenesis[5], and proliferation[6] of these cells. Gene expression of PAR-2 has been observed in adipose tissues and macrophages of humans and rats, and PAR-2 has been shown to promote inflammation and metabolic dysfunction[7]. Taken together, the results indicated the possibility that both PAR-1 and PAR-2 have a significant role in the development of insulin resistance. We and another group of researchers demonstrated that thrombin promotes the release of inflammatory cytokines and growth factors from adipocytes and inhibits insulin-stimulated Akt phosphorylation[8, 9]. We also showed that argatroban, a synthetic thrombin antagonist, can ameliorate insulin resistance in type 2 diabetic *db/db* mice[8]. Heparin cofactor II (HCII), like antithrombin, is a serine protease inhibitor (serpin) with a molecular weight of 65.6 kDa. HCII is synthesized by hepatocytes and secreted into the blood stream at a concentration of about 1.0 μmol/L[10]. HCII, upon activation by binding to dermatan sulfate proteoglycans, specifically inhibits thrombin action in various tissue matrices. Thus, HCII can inhibit thrombin action in various tissues without affecting hemostasis. Although we previously reported that HCII protects against cardiovascular remodeling in mice and humans[11-17], the role of HCII in the regulation of glucose metabolism and insulin sensitivity has not yet been determined. Therefore, the present study aimed to clarify whether HCII is involved in glucose metabolism and insulin sensitivity in humans and mice.

Materials and Methods

Subjects for Cross-Sectional Study

We determined the relationship between plasma HCII activity and HbA1c levels using data sets from our previous clinical studies[11, 13]. Additionally, a total of 130 individuals seeking consultation regarding lifestyle-related disorders and who had never been treated with insulin were recruited from Tokushima University Hospital, Tokushima, Japan between January 2012 and May 2013. All subjects underwent a standardized interview and physical examination.

Diagnostic Criteria for Clinical Studies

Current smokers were defined as subjects who had smoked within 1 year prior to the study. Body mass index was calculated as an index of obesity, and blood pressure was measured twice and averaged. Hypertensive patients were defined as those with systolic blood pressure ≥140 mmHg and/or diastolic blood pressure ≥90 mmHg, and individuals on antihypertensive medications. Hyperlipidemic patients were defined as those with low-density lipoprotein cholesterol (LDL-C) ≥140 mg/dl and/or triglyceride (TG) levels ≥150 mg/dl, and individuals on lipid-lowering medications. Diabetic patients were defined as individuals who were receiving oral hypoglycemic agents or individuals with glycosylated hemoglobin A1c (HbA1c) ≥6.5% or fasting plasma glucose (FPG) ≥126 mg/dl or 2 h plasma glucose ≥200 mg/dl during a 75 g oral glucose tolerance test. Exclusion criteria included overt cardiac failure, known malignancy, renal failure (serum creatinine ≥2.0 mg/dl), and malnutrition (serum albumin <3.0 g/dl).

Biochemical Analysis

Before noon, overnight fasting blood samples were collected from the antecubital vein and assayed immediately for FPG, HbA1c, serum immunoreactive insulin (IRI), and serum lipid parameters including TG, HDL-C, and LDL-C. FPG and levels of TG, HDL-C, LDL-C, and creatinine were measured by enzymatic methods. HbA1c was assayed by latex agglutination. Serum IRI level was determined by the chemiluminescent enzyme immunoassay. An index of insulin resistance in the homeostasis model assessment-insulin resistance (HOMA-IR) was calculated as FPG (mg/dl) × IRI (μU/ml)/405. For the measurements of plasma HCII activities, blood was drawn as described above, collected into a tube containing 1/10 volume of 3.8% sodium citrate, and centrifuged at 2,000 ×*g* for 20 min. Plasma was stored at −80℃ until use. Plasma HCII activity was measured on the basis of antithrombin activity in the presence of dermatan sulfate using the Stachrom® HCII assay kit (Diagnostica Stago, France). The intra-assay and inter-assay coefficients of variation of this kit were 3.9% and 4.3%, respectively. Our study followed the institutional guidelines of Tokushima University and was approved by the Institutional Review Board of Tokushima University Hospital. The ethics committee approved this study and the participants were required to sign an informed consent form prior to inclusion in the study, in accordance with the Declaration of Helsinki.

Animal Preparations

We used *HCII*^{+/+} and *HCII*^{+/−} 25-week-old male

Advance Publication
Journal of Atherosclerosis and Thrombosis
Accepted for publication: March 28, 2017
Published online: May 15, 2017

Heparin Cofactor Ⅱ and Hyperglycemia

mice (*HCⅡ*$^{+/-}$; Tokushima University, Graduate School of Biomedical Sciences, Tokushima, Japan) that we previously generated[12]. In brief, we generated *HCⅡ*-deficient mice by targeted disruption of the *HCⅡ* gene[12]. *HCⅡ*$^{+/-}$ mice were backcrossed for 10 generations with the C57BL/6J strain[12]. Because the homozygotic *HCⅡ*-deficient mice were embryonic lethal, we used male heterozygote *HCⅡ*-deficient (*HCⅡ*$^{+/-}$) mice and male littermate WT (*HCⅡ*$^{+/+}$) mice in all experiments of this study, as in our previous studies[12, 14, 17]. These animals were housed in a specific pathogen-free facility under climate-controlled conditions with a 12-h light/12-h dark cycle and were provided with either a normal diet (ND) or a high-fat diet (HFD: lard 58%, fish flour 30%, defatted soybean 10%, vitamins and minerals 2%) (Oriental Yeast Co., Ltd., Tokyo, Japan) and water ad libitum.

Biochemical Analysis

Plasma glucose levels were enzymatically measured (Wako Chemicals, Tokyo, Japan). Serum insulin levels, adiponectin levels, and leptin levels were determined using an insulin ELISA kit (Morinaga Institute of Biological Science, Inc., Japan), an adiponectin ELISA kit (Ohtsuka Pharmaceutical, Co, Ltd., Japan) and a leptin ELISA kit (Morinaga Institute of Biological Science, Inc., Japan). HOMA-IR was calculated as fasting whole blood glucose (mg/dl) × fasting serum insulin (ng/ml)/405.

Computed Tomography Scan

The adiposity of the mice was determined using computed tomography (CT) scanning at 25 weeks of age. Mice were anesthetized with isoflurane gas, and images were acquired on a Latheta LCT-200 (Hitachi Aloka Medical, Ltd. Japan) at Tokushima Bioimaging Station, The University of Tokushima. Animals were scanned in a 48-mm-wide specimen holder with a resolution of 96 µm pixels. For all scans, the same number of views (796) was used, which represents the amount of data collected during a single 360° rotation around the object. In pilot experiments, optimal scanning conditions were evaluated for each tissue. Obtained CT images were analyzed with provided software. Density histograms of the volume within the selected range were generated, and the total volume of skeletal muscle and adipose tissue were calculated by the summation of the total density.

Adipocyte Sizing

Epididymal fat samples were fixed in osmium tetroxide (Sigma), suspended in isotonic saline, and passed through a 250-µm nylon filter to remove fibrous elements. Cells were filtered over a 25-µm nylon filter, collected in isotonic saline, and analyzed on a Coulter counter (Mulisizer Ⅲ, Coulter Electronics, Fullerton, CA), as previously described[18]. The distribution of adipocyte size was analyzed for cells ranging 25−250 µm in diameter.

Immunohistochemistry

Mice were sacrificed by intraperitoneal injection of high-dose pentobarbital. White adipose tissues of epididymal fat were fixed overnight in 10% neutral buffered formalin, cut into 10-µm-thick cross sections, and stained with hematoxylin-eosin and F4/80 antibody (Santa Cruz Biotechnology Inc., Santa Cruz, CA). Antibody distribution was visualized with the avidin−biotin complex technique and Vector Red substrate (Vector Laboratories, Burlingame, CA). The summation of F4/80-positive cell numbers from five independent visual fields in each animal tissue was used to determine macrophage infiltration.

Quantitative Real-Time PCR and PCR Array Analysis

For real-time PCR analysis, epididymal fat tissues and hepatic tissues were excised. RNA extraction and reverse transcriptase-polymerase chain reactions (RT-PCR) were performed as previously described[12, 19]. In brief, epididymal fat tissues, hepatic tissues, and thigh skeletal muscle were homogenized in TRIzol (Invitrogen, Carlsbad, CA), and total RNA was extracted. One microgram of total RNA was used for cDNA synthesis with a QuantiTect Reverse Transcription Kit (QIAGEN, Valencia, CA), according to the manufacturer's instructions. The PCR mixture contained cDNA, synthesized from 2.5 ng of total RNA, 0.1 nmol/L forward and reverse primer mix, and SYBR Green (Platinum SYBR Green qPCR SuperMi-UDG, Invitrogen Carlsbad, CA). Assays were performed with a 7300 Real-Time PCR System (Applied Biosystems, Foster City, CA). Amplification consisted of one stage of 2 min at 50℃ and one stage of 2 min at 95℃ followed by 40 cycles of a 2-step cycle: 15 s at 95℃ and 30 s at 60℃. Quantitative RT-PCR analysis of 84 obesity-related genes was performed using Obesity RT^2 Profiler PCR Arrays PAMM-017Z (QIAGEN). Data analysis of the PCR array kit was performed using the manufacturer's integrated web-based software for the PCR Array System (http://pcrdataanalysis.sabiosciences.com/pcr/arrayanalysis.php) using $\Delta\Delta C_t$-based fold-change calculations. In addition, commercially available PCR primers were purchased from Perfect real-time primer (TAKARA BIO INC., Ohtsu, Japan) for *F2r*, *Mcp1*, *Tnf*, *Cntf*, *Cntfr*, *Pck1*, *G6pc*, and *Gapdh*. The transcript levels of those genes were adjusted relative to *Gapdh* expression as an internal control.

Table 1. Clinical characteristics of subjects and multiple regression analysis for determinants of HbA1c, FPG and HOMA-IR

Variables	mean ± SD	HbA1c		FPG		HOMA-IR	
		coefficient	p-value	coefficient	p-value	coefficient	p-value
Age (y.r.)	63.1 ± 9.9	0.018	0.053	0.482	0.037	0.008	0.487
Male/Female (n)	60/70	−0.029	0.891	5.389	0.312	−0.052	0.844
BMI (kg/m²)	24.8 ± 4.1	0.027	0.238	0.826	0.150	0.130	0.001
SBP (mmHg)	133.9 ± 20.3	0.007	0.153	0.166	0.196	0.000	0.045
LDL-C (mg/dl)	129.0 ± 30.5	0.004	0.212	0.072	0.321	0.004	0.311
HDL-C (mg/dl)	61.3 ± 16.1	−0.009	0.120	−0.186	0.213	−0.014	0.060
TG (mg/dl)	120.3 ± 69.6	0.000	0.731	0.018	0.581	0.000	0.790
UA (mg/dl)	5.4 ± 1.4	−0.064	0.388	−1.398	0.461	−0.091	0.361
Cre (mg/dl)	0.73 ± 0.17	−0.496	0.493	−19.329	0.293	0.202	0.830
FPG (mg/dl)	108.6 ± 22.2						
HbA1c (%)	6.2 ± 0.9						
HOMA-IR	1.71 ± 1.68						
HCII activities (%)	99.4 ± 18.4	−0.011	0.014	−0.311	0.007	−0.013	0.041
Current Smoking (%)	10.8% (14)	−0.105	0.662	−3.999	0.541	−0.058	0.864
Hypertension (%)	59.2% (77)	−0.090	0.673	−2.772	0.608	−0.165	0.547
Hyperlipidemia (%)	60.8% (79)	−0.182	0.345	−2.598	0.593	−0.000	0.486
Diabetes Mellitus (%)	30.0% (39)						

BMI: body mass index, SBP: systolic blood pressure, LDL-C: low density lipoprotein cholesterol, HDL-C: high density lipoprotein cholesterol, TG: triglyceride, UA: uric acid, Cre: creatinine, FPG: fasting plasma glucose, HbA1c: glycosylated hemoglobin A1c, HOMA: homeostatic model assessment, HCII: heparin cofactor II

Western Blot Analysis

For western blot analysis, murine epididymal fat tissues, hepatic tissues, and thigh skeletal muscle were excised. The phosphorylation of AMPKα and Akt with or without insulin stimulation (1 U/kg) was evaluated by western blot analysis. Protein extraction and western blot analysis were performed as previously described [17, 19]. In brief, 100-μg protein extracts from adipose tissue, hepatic tissues, and thigh skeletal muscle from $HCII^{+/+}$ and $HCII^{+/-}$ mice fed an ND or HFD were boiled for 5 min in Laemmli sample buffer and run on SDS-PAGE. The protein extracts were then transferred to a PVDF membrane (Millipore Corporation, Bedford, MA). The membrane was blocked for 20 min at room temperature with SuperBlock T20 TBS Blocking Buffer (Thermo Scientific, Rockford, IL). The blots were incubated overnight at 4℃ with each primary antibody, followed by incubation for 1 h with anti-rabbit secondary antibody (horseradish peroxidase-conjugated). Immunoreactive bands were visualized using enhanced chemiluminescence with ECL-PLUS reagents (GE Healthcare, Buckinghamshire, UK) and exposure to a lumino image analyzer (LAS-3000 mini) (Fujifilm Corporation, Tokyo, Japan). The signals were quantified by densitometry using ImageJ version 1.47. About 8−12 independent samples were analyzed in each group, and the phosphospecific pro-teins were corrected by GAPDH as an internal control. We used primary antibodies against phosphory-lated Akt (Ser473), phosphorylated AMPK (Thr172), and GAPDH (Cell Signaling Technology, Beverly, MA). All experimental procedures were performed in accordance with the guidelines from and approval of the Animal Research Committee of The University of Tokushima Graduate School.

Statistical Analysis

In the clinical study, continuous variables were averaged; values were expressed as mean ± SD or as percentages for categorical parameters. Male gender, presence of hypertension, diabetes mellitus, hyperlipidemia, and current smoking were coded as dummy variables. The degree of association among independent variables for each glucose metabolism marker was assessed by multiple regression analysis. In the animal study, values for each parameter within a group are expressed as dot plots with mean bars. The Kruskal−Wallis test was used to assess the statistical significance of quantitative data among the groups. Bonferroni-corrected Mann−Whitney U test or Dunn test was used for multiple comparisons. Statistical significance was set at $p < 0.05$.

Advance Publication
Journal of Atherosclerosis and Thrombosis
Accepted for publication: March 28, 2017
Published online: May 15, 2017

Heparin Cofactor II and Hyperglycemia

A Y=-0.011X+6.854
R^2=0.060, p<0.01

B Y=-0.128X+115.85
R^2=0.041, p<0.05

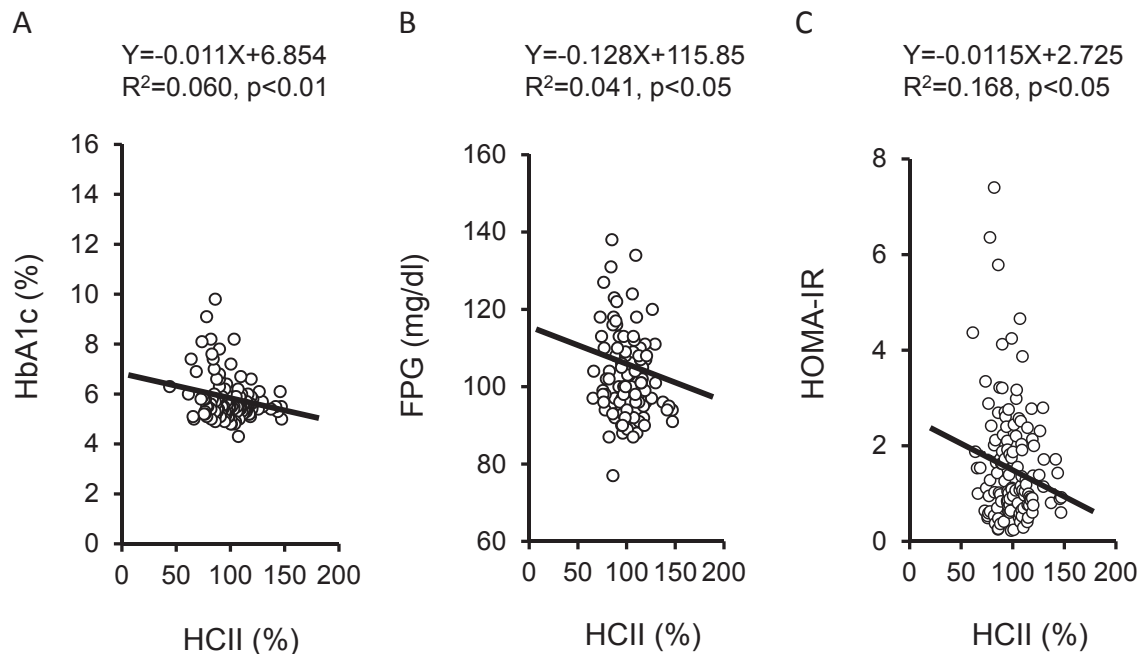C Y=-0.0115X+2.725
R^2=0.168, p<0.05

Fig. 1. Scatter plots of plasma HCII activity and HbA1c values (A), plasma HCII activity and FPG levels (B), and of plasma HCII activity and HOMA-IR values (C) (n = 130 in each panel).

Results

Plasma HCII Activity is Inversely Associated with HbA1c, FPG, and HOMA-IR in Humans

We used clinical data sets from our previous studies[11, 13] and 130 newly recruited elderly Japanese subjects. The clinical characteristics of subjects from our previous studies, the present study, and the subjects in both studies are shown in **Table 1**, **Supplemental Table 1** and **Supplemental Table 2**. Scatter plots of plasma HCII activities and glycosylated hemoglobin A1c (HbA1c) in each of the three studies showed significant inverse relationships (**Fig. 1A**, **Supplemental Figs. 1A**, **1B**, & **1C**); this was also found when combining data from the three studies (**Supplemental Fig. 1D**). Significant inverse relationships were also found between HCII activity and FPG (**Fig. 1B**), and between HCII activity and HOMA-IR (**Fig. 1C**). Multiple regression analysis confirmed inverse correlations between plasma HCII activity and HbA1c, plasma HCII activity and FPG, and plasma HCII activities and HOMA-IR, even after adjustment for age, sex, and other confounding factors (**Table 1**).

HFD Prominently Increases Adipocyte Size in *HCII*$^{+/-}$ Mice

To examine whether the inhibition of thrombin action by HCII plays a role in the regulation of glucose metabolism, we used *HCII*$^{+/-}$ mice and compared their glucose metabolism with that of *HCII*$^{+/+}$ mice. Growth curve analysis revealed no difference between *HCII*$^{+/+}$ and *HCII*$^{+/-}$ mice fed ND (**Fig. 2A**). Both *HCII*$^{+/+}$ and *HCII*$^{+/-}$ mice who were fed HFD showed greater increase in body weight compared to mice who were fed ND (**Fig. 2A**). Body composition assessment by CT revealed no significant differences in the volume of skeletal muscles, subcutaneous fat, and visceral fat between *HCII*$^{+/+}$ and *HCII*$^{+/-}$ mice (**Figs. 2B**, **2C**, & **2D**). On the contrary, Coulter counter analysis revealed greater adipocyte diameters in HFD-fed *HCII*$^{+/-}$ mice than in HFD-fed *HCII*$^{+/+}$ mice (**Figs. 2E** & **2F**).

HFD-Induced Obesity Causes Greater Hyperglycemia and Hyperinsulinemia in *HCII*$^{+/-}$ Mice

Although no obvious difference in FPG was observed between *HCII*$^{+/+}$ and *HCII*$^{+/-}$ mice fed ND, higher FPG levels were observed in HFD-fed *HCII*$^{+/-}$ mice than that in HFD-fed *HCII*$^{+/+}$ mice (**Fig. 2G**). Fasting serum insulin levels more prominently increased in *HCII*$^{+/-}$ mice than in *HCII*$^{+/+}$ mice in the HFD group (**Fig. 2H**); this resulted in higher HOMA-IR values in *HCII*$^{+/-}$ mice than those in *HCII*$^{+/+}$ mice in the HFD group (**Fig. 2I**). There were no significant differences in adiponectin or leptin serum levels between *HCII*$^{+/+}$ and *HCII*$^{+/-}$ mice in each diet group (**Figs. 3A** & **3B**).
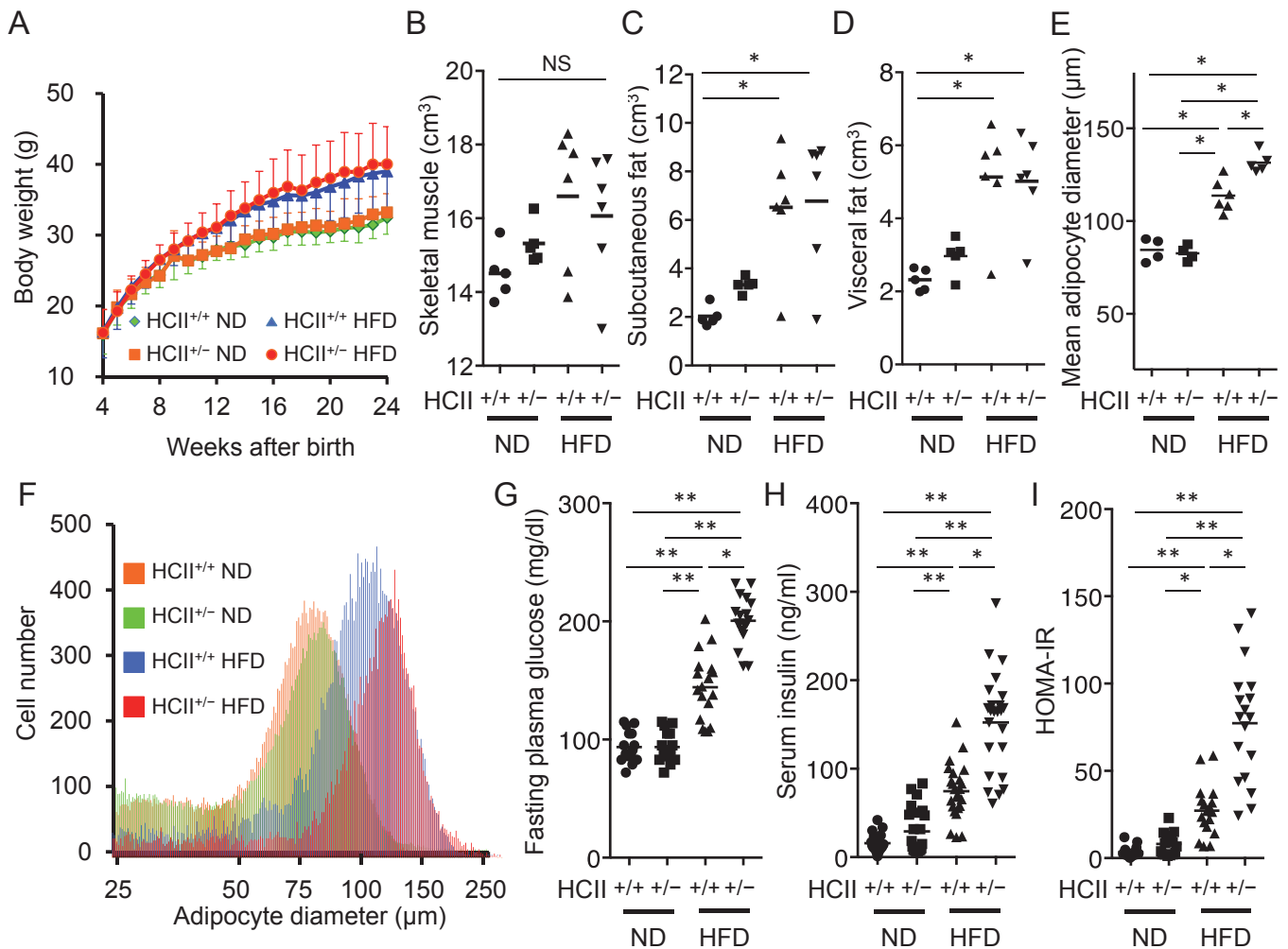
Fig. 2. Gross phenotype and aberrant glucose metabolism in HCII-deficient mice

(A) Growth curve analysis after weaning in $HCII^{+/+}$ and $HCII^{+/-}$ mice fed ND or HFD ($n = 18$ in each group). Error bar indicates standard deviation. (B) Measurements of skeletal muscle volume, (C) subcutaneous fat volume, and (D) visceral fat volume by computed tomography scans in $HCII^{+/+}$ and $HCII^{+/-}$ mice fed ND or HFD ($n = 5-6$ in each group). (E) Coulter counter analysis for mean adipocyte (epididymal fat tissue) diameter measurements among the four mice groups ($n = 4-6$ in each group). (F) Representative results of Coulter counter analysis for measurements of adipocyte diameters among the four mice groups. (G) Measurements of fasting plasma glucose levels, (H) serum insulin levels and (I) HOMA-IR values in $HCII^{+/+}$ and $HCII^{+/-}$ mice fed ND or HFD ($n = 16-24$ in each group). Bars represent the mean values in each group. $*p < 0.05$, $**p < 0.01$

HFD Accelerates Inflammation and Macrophage Recruitment in the Adipose Tissue of $HCII^{+/-}$ Mice

In the quantitative RT-PCR analysis of epididymal fat tissue, no significant difference in the gene expression levels of $F2r$, a murine homologue of thrombin receptor gene, was observed (**Fig. 3C**). Because chronic inflammation in adipose tissue plays pivotal roles in the development of insulin resistance, we evaluated the gene expression levels of monocyte chemotactic protein-1 ($Mcp1$) and tumor necrosis factor (Tnf) in epididymal fat tissue in mice. The expression levels of $Mcp1$ and Tnf genes significantly increased in $HCII^{+/-}$ mice compared to those in $HCII^{+/+}$ mice in

the HFD group (**Figs. 3D** & **3E**). In addition, immunohistochemical analysis revealed that F4/80 (cell-surface marker of macrophages)-positive cells were significantly increased in $HCII^{+/-}$ mice fed HFD compared to other groups (**Figs. 3H** & **3I**). These results are consistent with the marked enhancement of $Mcp1$ and Tnf gene expression in $HCII^{+/-}$ mice with HFD-induced obesity (**Figs. 3D** & **3E**).

HCII Insufficiency Dysregulates the CNTF−CNTF Receptor Axis in Adipose Tissue of HFD-Treated Obese Mice

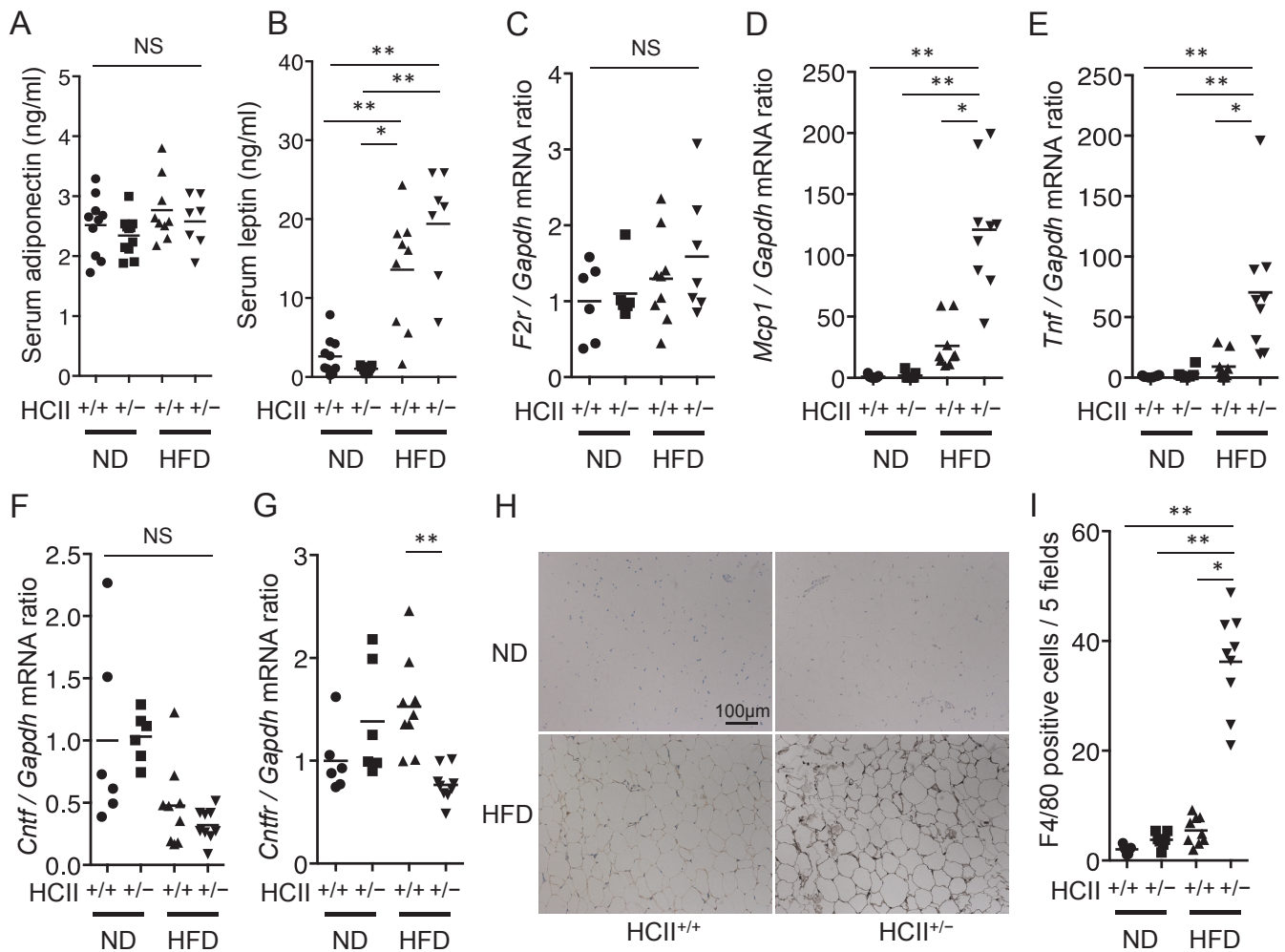To identify other glucose metabolism-related key

Advance Publication
Journal of Atherosclerosis and Thrombosis
Accepted for publication: March 28, 2017
Published online: May 15, 2017

Heparin Cofactor Ⅱ and Hyperglycemia

Fig. 3. Serum adiponectin and leptin levels, gene expression profiles, and macrophage infiltration in adipose tissues of $HCII^{+/+}$ and $HCII^{+/-}$ mice fed ND or HFD

(A) Serum levels of adiponectin and (B) leptin in $HCII^{+/+}$ and $HCII^{+/-}$ mice fed ND or HFD ($n=7-10$ in each group). (C) Gene expression levels of $F2r$, (D) $Mcp1$, (E) Tnf, (F) $Cntf$, and (G) $Cntfr$ in adipose tissues of $HCII^{+/+}$ and $HCII^{+/-}$ mice fed ND or HFD ($n=6-9$ in each group). (H) Representative photos of F4/80 staining and (I) quantification of total F4/80-positive cell numbers counted from the five independent visual fields in adipose tissues of $HCII^{+/+}$ and $HCII^{+/-}$ mice fed ND or HFD. Bars represent the mean values in each group. $*p<0.05$, $**p<0.01$

molecules, we screened the gene expression profiles in HFD-treated murine adipose tissues (epididymal fat tissue) with a PCR Array System, and found that ciliary neurotrophic factor receptor ($Cntfr$) was significantly downregulated in $HCII^{+/-}$ mice (**Supplemental Table 3**). Although $Cntf$ gene expression levels did not significantly differ between $HCII^{+/+}$ and $HCII^{+/-}$ mice, regardless of diet (**Fig. 3F**), $Cntfr$ gene expression was significantly reduced in $HCII^{+/-}$ mice compared to $HCII^{+/+}$ mice in the HFD group (**Fig. 3G**). However, in an *in vitro* study, we failed to prove that HCII and/or dermatan sulfate are able to increase both $Cntf$ and $Cntfr$ gene expression levels in adipocytes with statistical significance (**Supplemental Figs. 2A** & **2B**). These

results indicated that HCII seems to be indirectly associated with the CNTF−CNTF receptor axis *in vivo*.

HCII Insufficiency Reduces Phosphorylation of Akt and AMPK in the Adipose Tissue of Obese Mice

We investigated the phosphorylation of AMPK in adipose tissues (epididymal fat tissue), liver, and skeletal muscle of $HCII^{+/+}$ and $HCII^{+/-}$ mice. Western blot analysis demonstrated that HFD-fed $HCII^{+/-}$ mice had reduced the phosphorylation of AMPK in adipose tissue but not in the liver and skeletal muscle, compared with HFD-fed $HCII^{+/+}$ mice (**Fig. 4A** and **Supplemental Figs. 3A** & **3B**). In addition to AMPK,

Advance Publication
Journal of Atherosclerosis and Thrombosis
Accepted for publication: March 28, 2017
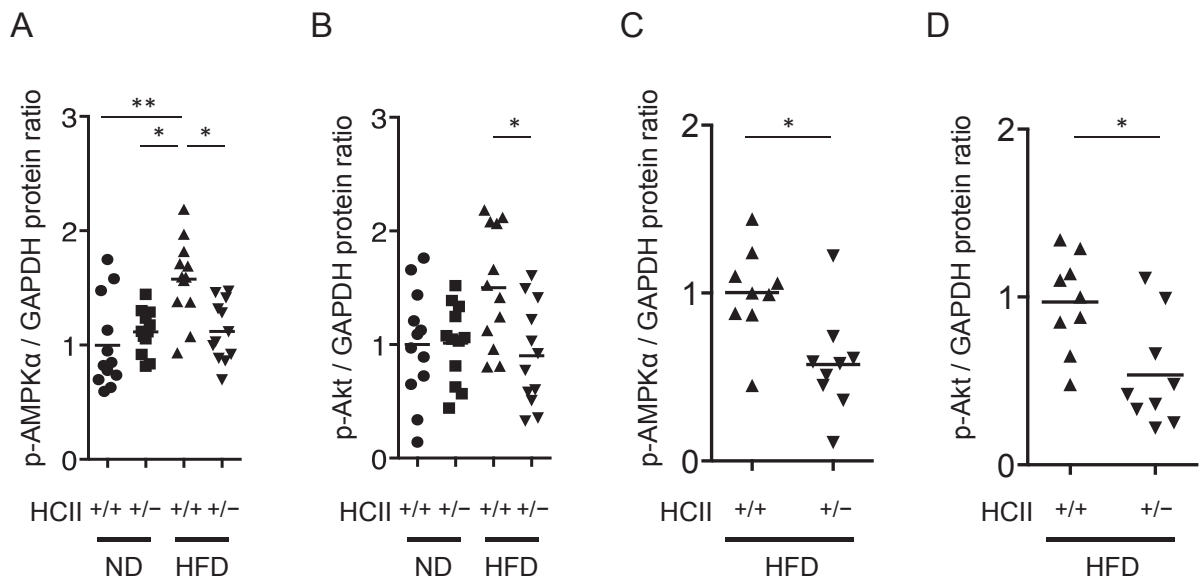Published online: May 15, 2017

Kurahashi *et al.*

Fig. 4. Aberrant phosphorylation of insulin resistance-related factors

Results of western blot analysis for GAPDH-adjusted phosphorylated AMPK (A) and phosphorylated Akt (B) in adipose tissues of $HCII^{+/+}$ and $HCII^{+/-}$ mice fed ND or HFD ($n = 12$ in each group). Results of western blot analysis for GAPDH-adjusted phosphorylated AMPK (C) and phosphorylated Akt (D) in the adipose tissues of $HCII^{+/+}$ and $HCII^{+/-}$ mice fed HFD after insulin injection ($n = 9$ in each group). $*p < 0.05$, $**p < 0.01$

we examined whether obese $HCII^{+/-}$ mice have aberrant Akt phosphorylation in their adipose tissue, liver, and skeletal muscle. In the present study, HFD-fed $HCII^{+/-}$ mice exhibited insufficient phosphorylation of Akt in adipose tissue but not in liver and skeletal muscle, compared to HFD-fed $HCII^{+/+}$ mice (**Fig. 4B** and **Supplemental Figs. 3A** & **3B**). Moreover, we observed that insulin-stimulated phosphorylation of AMPKα and Akt in adipose tissue of HFD-treated $HCII^{+/-}$ mice was also reduced compared to that in HFD-treated $HCII^{+/+}$ mice (**Figs. 4C** & **4D**). From these results, it is plausible to assume that both Akt and AMPK inactivation in the adipose tissue of $HCII^{+/-}$ mice impair glucose transport and insulin action.

HFD Enhances the Expression of Gluconeogenesis-Related Genes in $HCII^{+/-}$ Mice

Gluconeogenesis is regulated by the activity of two rate-limiting enzymes, phosphoenolpyruvate carboxykinase (PEPCK) and glucose-6-phosphatase (G6 Pase)[20]. Therefore, we examined the expression levels of these genes in the liver, and found that mRNA levels of both *Pck1* (murine PEPCK homolog) and *G6pc* (murine G6 Pase homolog) in HFD-fed $HCII^{+/-}$ mice were higher than those in HFD-fed $HCII^{+/+}$ mice (**Figs. 5A** and **5B**).

Discussion

In the present study, we provide the first evidence that plasma HCII activity is inversely associated with FPG, HbA1c, and HOMA-IR in humans. Furthermore, fasting hyperglycemia and prominent insulin resistance were more frequently found in HFD-fed $HCII^{+/-}$ mice than that in HFD-fed $HCII^{+/+}$ mice.

Obesity-induced glucose metabolism disorder is recognized as chronic low-grade systemic inflammation. Recently, molecular bases of metabolic inflammation and their potential pathogenic roles in diabetes and cardiovascular disease have been investigated[21-23]. Increasing evidence has revealed that the chemokine system is involved in chronic inflammation leading to obesity, insulin resistance, and T2DM. In this regard, MCP-1 is considered to play a pivotal role in obesity-induced insulin resistance[24]. In our previous study, we found that *Mcp1* gene expression in 3T3-L1 adipocytes is markedly increased by thrombin treatment, suggesting that thrombin is a key molecule linking increased adiposity and an enhanced expression of MCP-1[8]. In addition, we previously demonstrated that cuff injury of femoral arteries in $HCII^{+/-}$ mice prominently augmented neointimal hyperplasia with the enhancement of vascular *Mcp1* gene expression[12]. Therefore, HCII may be closely associated with the regulation of thrombin-MCP-1 axis.

TNF-α has also been recognized as a key mole-

Advance Publication
Journal of Atherosclerosis and Thrombosis
Accepted for publication: March 28, 2017
Published online: May 15, 2017

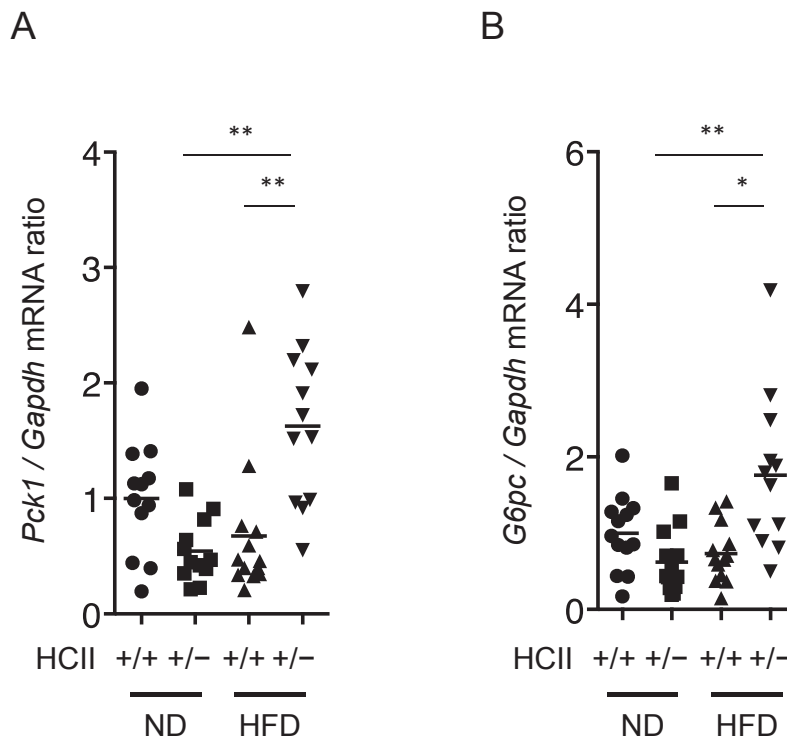Heparin Cofactor II and Hyperglycemia

Fig. 5. Enhanced gene expression of gluconeogenesis-related factors in HFD-treated *HCII*^{+/−} mice

Gene expression levels of *Pck1* (A) and *G6pc* (B) in hepatic tissues of *HCII*^{+/+} and *HCII*^{+/−} mice fed ND or HFD (*n* = 12 or 13 in each group). Bars represent the mean values in each group. *$p < 0.05$, **$p < 0.01$

cule linking obesity and insulin resistance. Because TNF-α is overexpressed in the adipose tissue of obese animals and humans, and because obese mice lacking either TNF-α or its receptor have attenuated insulin resistance[25], it is plausible that the prominent gene expression of *tnf* was observed in HFD-treated *HCII*^{+/−} mice with insulin resistance. Moreover, Kalle *et al.* reported that *HCII*-deficient mice exhibit increased susceptibility to *Pseudomonas aeruginosa* infection with elevated inflammatory plasma cytokines such as interleukin 6, TNF-α, MCP-1, and interferon-γ[26]. Their study suggested that HCII is an immunological regulator having broad anti-inflammatory effects. Taken together, these results are consistent with the notion that HCII deficiency promotes macrophage infiltration, leading to low-grade, chronic inflammation in adipose tissue.

In the present study, we found that *Cntfr* was significantly downregulated in *HCII*^{+/−} mice. CNTF is known to prevent obesity and ameliorate glucose tolerance. Watt *et al.* demonstrated that CNTF signals increase fatty acid oxidation and reduce insulin resistance via AMPK activation[27]. Although we observed a reduced ratio of *Cntf* to *Cntfr* gene expression in HFD-treated *HCII*^{+/−} mice, the detailed mechanism underlying the influence of serine protease and/or its inhibitor on CNTF−CNTF receptor axis has been largely unknown. However, our *in vivo* and *in vitro* experimental results suggest that the aberrant balance between *Cntf* and *Cntfr* gene expression levels in *HCII*^{+/−} mice may be indirectly correlated with impaired AMPK activation. In addition, the finding of reduced phosphorylation of AMPK in HFD-treated *HCII*^{+/−} mice is consistent with the results of our previous study showing that HCII deficiency causes impaired AMPK phosphorylation in ischemic skeletal muscle, leading to insufficient angiogenic response[17]. Thus, the present observations that reduced HCII activity leads to AMPK inactivation in adipose tissue may at least partly explain why *HCII*^{+/−} mice with HFD-induced obesity developed insulin resistance.

The serine/threonine protein kinase Akt is strongly associated with the homeostatic regulation of glucose metabolism[28]. Targeted disruption of PKBβ, an Akt isoform, in mice diminished the insulin-stimulated glucose uptake in muscle and adipocytes, and the dysregulation of hepatic glucose production[29]. As our previous study provided evidence that thrombin stim-

9

Advance Publication
Journal of Atherosclerosis and Thrombosis
Accepted for publication: March 28, 2017
Published online: May 15, 2017

ulation blunts Akt phosphorylation in 3T3L-1 adipocytes[8], we evaluated Akt phosphorylation in the adipose tissue of mice and found that HCII deficiency causes insufficient activation of Akt in HFD-induced obesity. It has been demonstrated that macrophage infiltration and secreted factors from the macrophages in adipocytes inhibit Akt phosphorylation, subsequently impairing insulin action[30]. The enhancement of macrophage infiltration along with increased gene expression of *Mcp1* induced by HCII deficiency may partially explain Akt inactivation. From these results, it is plausible to assume that Akt inactivation, along with AMPK inactivation, in the adipose tissue of $HCII^{+/-}$ mice impair glucose transport and insulin action.

Gluconeogenesis is one of the major mechanisms to maintain blood glucose levels and prevent hypoglycemia. The acceleration of gluconeogenesis in the liver is largely responsible for fasting hyperglycemia in patients with T2DM[31]. Gluconeogenesis is regulated by the activity of two rate-limiting enzymes, PEPCK and G6 Pase[20]. Therefore, we evaluated the expression levels of these genes in the liver, and found that the mRNA levels of both *Pck1* (murine PEPCK homologue) and *G6pc* (murine G6 Pase homologue) in HFD-fed $HCII^{+/-}$ mice were higher than those in HFD-fed $HCII^{+/+}$ mice. Previous studies showed that thrombin activates NAD(P)H oxidase; oxidative stress is known to be associated with increased expression of PEPCK and G6 Pase. Thus, it is possible that HCII deficiency augments oxidative stress by activating the tissue thrombin-PAR-1 axis and enhances PEPCK and G6 Pase expression, leading to fasting hyperglycemia.

Oxidative stress and chronic inflammation are known to be associated with the development of metabolic diseases, including obesity and diabetes[32]. Because we previously reported that $HCII^{+/-}$ mice manifest excessive superoxide production at the sites of vascular injury, the observed glucose metabolism disorder in the present study may be associated with an abnormal oxidative stress state in HFD-treated $HCII^{+/-}$ mice.

As thrombin inactivation is effectively caused by complex formation with HCII and dermatan sulfate (DS), DS has an important role in the modulation of thrombin action. Because glycosaminoglycans (GAGs) undergo structural and functional remodeling in various pathological states including hyperglycemia and the levels of GAGs such as chondroitin/DS are significantly decreased in diabetic condition[33, 34], the amount and functional changes of DS may be associated with thrombin inhibition by HCII.

In conclusion, the present study provides evidence supporting the assumption that HCII, a serine protease inhibitor, plays an important role in maintaining glucose homeostasis by regulating insulin sensitivity in both humans and mice. Our findings suggest that the measurement of plasma HCII activity may be useful for identifying patients at high risk for T2DM and cardiovascular complications. In addition, the stimulation of HCII production may be a novel therapeutic approach to ameliorate cardiovascular diseases and diabetic conditions in patients with T2DM.

Conflicts of Interest/Disclosures

The authors report no conflicts of interest or disclosures.

Acknowledgments/Sources of Funding

References

1) Samad F and Ruf W. Inflammation, obesity, and thrombosis. Blood. 2013; 122: 3415-3422
2) Sanchez C, Poggi M, Morange PE, Defoort C, Martin JC, Tanguy S, Dutour A, Grino M and Alessi MC. Diet modulates endogenous thrombin generation, a biological estimate of thrombosis risk, independently of the metabolic status. Arterioscler Thromb Vasc Biol. 2012; 32: 2394-2404
3) McNamara CA, Sarembock IJ, Gimple LW, Fenton JW, 2nd, Coughlin SR and Owens GK. Thrombin stimulates proliferation of cultured rat aortic smooth muscle cells by a proteolytically activated receptor. J Clin Invest. 1993; 91: 94-98
4) Derian CK, Damiano BP, D'Andrea MR and Andrade-Gordon P. Thrombin regulation of cell function through protease-activated receptors: implications for therapeutic intervention. Biochemistry (Mosc). 2002; 67: 56-64
5) Griffin CT, Srinivasan Y, Zheng YW, Huang W and Coughlin SR. A role for thrombin receptor signaling in endothelial cells during embryonic development. Science. 2001; 293: 1666-1670
6) Cheung WM, D'Andrea MR, Andrade-Gordon P and Damiano BP. Altered vascular injury responses in mice deficient in proteaseactivated receptor-1. Arterioscler Thromb Vasc Biol. 1999; 19: 3014-3024
7) Lim J, Iyer A, Liu L, Suen JY, Lohman RJ, Seow V, Yau MK, Brown L and Fairlie DP. Diet-induced obesity, adipose inflammation, and metabolic dysfunction correlating with PAR2 expression are attenuated by PAR2 antagonism. FASEB J. 2013; 27: 4757-4767
8) Mihara M, Aihara K, Ikeda Y, Yoshida S, Kinouchi M, Kurahashi K, Fujinaka Y, Akaike M and Matsumoto T. Inhibition of thrombin action ameliorates insulin resistance in type 2 diabetic db/db mice. Endocrinology. 2010; 151: 513-519

Advance Publication
Journal of Atherosclerosis and Thrombosis
Heparin Cofactor Ⅱ and Hyperglycemia
Accepted for publication: March 28, 2017
Published online: May 15, 2017

9) Strande JL and Phillips SA. Thrombin increases inflammatory cytokine and angiogenic growth factor secretion in human adipose cells in vitro. J Inflamm. 2009; 6: 4

10) Tollefsen DM, Pestka CA and Monafo WJ. Activation of heparin cofactor Ⅱ by dermatan sulfate. J Biol Chem. 1983; 258: 6713-6716

11) Aihara K, Azuma H, Takamori N, Kanagawa Y, Akaike M, Fujimura M, Yoshida T, Hashizume S, Kato M, Yamaguchi H, Kato S, Ikeda Y, Arase T, Kondo A and Matsumoto T. Heparin cofactor Ⅱ is a novel protective factor against carotid atherosclerosis in elderly individuals. Circulation. 2004; 109: 2761-2765

12) Aihara K, Azuma H, Akaike M, Ikeda Y, Sata M, Takamori N, Yagi S, Iwase T, Sumitomo Y, Kawano H, Yamada T, Fukuda T, Matsumoto T, Sekine K, Sato T, Nakamichi Y, Yamamoto Y, Yoshimura K, Watanabe T, Nakamura T, Oomizu A, Tsukada M, Hayashi H, Sudo T, Kato S and Matsumoto T. Strain-dependent embryonic lethality and exaggerated vascular remodeling in heparin cofactor Ⅱ-deficient mice. J Clin Invest. 2007; 117: 1514-1526

13) Aihara K, Azuma H, Akaike M, Kurobe H, Takamori N, Ikeda Y, Sumitomo Y, Yoshida S, Yagi S, Iwase T, Ishikawa K, Sata M, Kitagawa T and Matsumoto T. Heparin cofactor Ⅱ is an independent protective factor against peripheral arterial disease in elderly subjects with cardiovascular risk factors. J Atheroscler Thromb. 2009; 16: 127-134

14) Sumitomo-Ueda Y, Aihara K, Ise T, Yoshida S, Ikeda Y, Uemoto R, Yagi S, Iwase T, Ishikawa K, Hirata Y, Akaike M, Sata M, Kato S and Matsumoto T. Heparin cofactor Ⅱ protects against angiotensin Ⅱ-induced cardiac remodeling via attenuation of oxidative stress in mice. Hypertension. 2010; 56: 430-436

15) Takamori N, Azuma H, Kato M, Hashizume S, Aihara K, Akaike M, Tamura K and Matsumoto T. High plasma heparin cofactor Ⅱ activity is associated with reduced incidence of in-stent restenosis after percutaneous coronary intervention. Circulation. 2004; 109: 481-486

16) Ise T, Aihara K, Sumitomo-Ueda Y, Yoshida S, Ikeda Y, Yagi S, Iwase T, Yamada H, Akaike M, Sata M and Matsumoto T. Plasma heparin cofactor Ⅱ activity is inversely associated with left atrial volume and diastolic dysfunction in humans with cardiovascular risk factors. Hypertens Res. 2011; 34: 225-231

17) Ikeda Y, Aihara K, Yoshida S, Iwase T, Tajima S, Izawa-Ishizawa Y, Kihira Y, Ishizawa K, Tomita S, Tsuchiya K, Sata M, Akaike M, Kato S, Matsumoto T and Tamaki T. Heparin cofactor Ⅱ, a serine protease inhibitor, promotes angiogenesis via activation of the AMP-activated protein kinase-endothelial nitric-oxide synthase signaling pathway. J Biol Chem. 2012; 287: 34256-34263

18) Sakai T, Sakaue H, Nakamura T, Okada M, Matsuki Y, Watanabe E, Hiramatsu R, Nakayama K, Nakayama KI and Kasuga M. Skp2 controls adipocyte proliferation during the development of obesity. J Biol Chem. 2007; 282: 2038-2046

19) Yoshida S, Aihara K, Ikeda Y, Sumitomo-Ueda Y, Uemoto R, Ishikawa K, Ise T, Yagi S, Iwase T, Mouri Y, Sakari M,

Matsumoto T, Takeyama K, Akaike M, Matsumoto M, Sata M, Walsh K, Kato S and Matsumoto T. Androgen receptor promotes sex-independent angiogenesis in response to ischemia and is required for activation of vascular endothelial growth factor receptor signaling. Circulation. 2013; 128: 60-71

20) Yabaluri N and Bashyam MD. Hormonal regulation of gluconeogenic gene transcription in the liver. J Biosci. 2010; 35: 473-484

21) Hansson GK and Libby P. The immune response in atherosclerosis: a double-edged sword. Nat Rev Immunol. 2006; 6: 508-519

22) Shoelson SE, Lee J and Goldfine AB. Inflammation and insulin resistance. J Clin Invest. 2006; 116: 1793-1801

23) Hotamisligil GS. Inflammation and metabolic disorders. Nature. 2006; 444: 860-867

24) Ota T. Chemokine systems link obesity to insulin resistance. Diabetes & metabolism journal. 2013; 37: 165-172

25) Nieto-Vazquez I, Fernandez-Veledo S, Kramer DK, Vila-Bedmar R, Garcia-Guerra L and Lorenzo M. Insulin resistance associated to obesity: the link TNF-alpha. Arch Physiol Biochem. 2008; 114: 183-194

26) Kalle M, Papareddy P, Kasetty G, Tollefsen DM, Malmsten M, Morgelin M and Schmidtchen A. Proteolytic activation transforms heparin cofactor Ⅱ into a host defense molecule. J Immunol. 2013; 190: 6303-6310

27) Watt MJ, Dzamko N, Thomas WG, Rose-John S, Ernst M, Carling D, Kemp BE, Febbraio MA and Steinberg GR. CNTF reverses obesity-induced insulin resistance by activating skeletal muscle AMPK. Nat Med. 2006; 12: 541-548

28) Kohn AD, Barthel A, Kovacina KS, Boge A, Wallach B, Summers SA, Birnbaum MJ, Scott PH, Lawrence JC, Jr. and Roth RA. Construction and characterization of a conditionally active version of the serine/threonine kinase Akt. J Biol Chem. 1998; 273: 11937-11943

29) Dummler B and Hemmings BA. Physiological roles of PKB/Akt isoforms in development and disease. Biochem Soc Trans. 2007; 35: 231-235

30) Lumeng CN, Deyoung SM and Saltiel AR. Macrophages block insulin action in adipocytes by altering expression of signaling and glucose transport proteins. Am J Physiol Endocrinol Metab. 2007; 292: E166-E174

31) Taylor SI. Deconstructing type 2 diabetes. Cell. 1999; 97: 9-12

32) Newsholme P, Cruzat VF, Keane KN, Carlessi R and de Bittencourt PI, Jr. Molecular mechanisms of ROS production and oxidative stress in diabetes. Biochem J. 2016; 473: 4527-4550

33) Joladarashi D, Salimath PV and Chilkunda ND. Diabetes results in structural alteration of chondroitin sulfate/dermatan sulfate in the rat kidney: effects on the binding to extracellular matrix components. Glycobiology. 2011; 21: 960-972

34) Gowd V, Gurukar A and Chilkunda ND. Glycosaminoglycan remodeling during diabetes and the role of dietary factors in their modulation. World J Diabetes. 2016; 7: 67-73

Kurahashi et al.

Supplemental Table 1.

Characteristics	Total ($n=306$)	Men ($n=154$)	Women ($n=152$)	p-value
Age (yr)	68.9 ± 11.1	67.2 ± 10.8	70.6 ± 11.1	< 0.01
Body mass index (kg/m²)	23.2 ± 3.7	23.6 ± 3.8	22.8 ± 3.5	NS
SBP (mmHg)	138.3 ± 20.2	138.2 ± 20.2	138.5 ± 20.3	NS
Total cholesterol (mg/dL)	198.1 ± 39.6	187.3 ± 40.9	209.1 ± 35.1	< 0.0001
LDL-cholesterol (mg/dL)	124.5 ± 34.5	114.4 ± 35.5	134.8 ± 30.3	< 0.0001
HDL-cholesterol (mg/dL)	47.0 ± 13.2	44.2 ± 12.4	49.9 ± 13.4	< 0.0005
Triglyceride (mg/dL)	131.6 ± 85.4	143.5 ± 104.1	119.5 ± 58.8	< 0.05
Lipid peroxide (nmol/mL)	0.45 ± 0.23	0.48 ± 0.26	0.41 ± 0.18	< 0.005
Lipoprotein(a) (mg/dL)	23.0 ± 17.1	22.9 ± 15.7	23.1 ± 18.5	NS
HbA1c (%)	5.9 ± 1.7	6.1 ± 1.8	5.8 ± 1.6	NS
Antithrombin activity (%)	93.1 ± 14.8	89.5 ± 14.3	96.6 ± 14.5	< 0.0005
Heparin cofactor II activity (%)	94.0 ± 18.3	92.1 ± 18.2	95.9 ± 18.2	NS
Maximum plaque thickness (mm)	2.04 ± 1.13	2.15 ± 1.18	1.93 ± 1.07	NS
Current smoking (%)	28.4	48.7	7.9	< 0.0001
Hypertension (%)	57.8	55.8	59.9	NS
Hyperlipidemia (%)	42.5	35.7	49.3	< 0.05
Diabetes mellitus (%)	30.7	36.4	25	< 0.05

Values are means ± SD or percentages.
Baseline characteristics were compared between men and women by unpaired t test or χ^2 test for independence.
(Referred from the article by Aihara *et al*. Circulation. 2004; 109: 2761-2765)

Supplemental Table 2.

Characteristics	ABI ≥ 0.9 ($n=432$)	ABI < 0.9 ($n=62$)	p-value (ABI ≥ 0.9 vs < 0.9)
Male/Female	233/199	41/21	0.065
Age (yr)	66.4 ± 11.0	71.0 ± 9.5	0.001
BMI (kg/m²)	23.7 ± 3.5	22.4 ± 2.8	0.001
SBP (mmHg)	136.2 ± 20.5	143.6 ± 20.4	0.001
LDL-cholesterol (mg/dL)	121.0 ± 35.0	129.2 ± 40.8	0.134
HDL-cholesterol (mg/dL)	50.9 ± 16.9	50.7 ± 24.0	0.938
Triglyceride (mg/dL)	139.4 ± 86.2	136.2 ± 78.2	0.762
Lipoprotein(a) (mg/dL)	20.7 ± 15.8	27.0 ± 27.4	0.081
HbA1c (%)	6.0 ± 1.7	7.3 ± 6.7	0.148
Antithrombin activity (%)	97.8 ± 15.8	94.7 ± 17.0	0.173
Heparin cofactor II activity (%)	94.6 ± 17.8	87.5 ± 19.7	0.009
Current smoking (%)	127 (29.4)	23 (41.1)	0.003
Hypertension (%)	266 (61.6)	46 (74.2)	0.041
Hyperlipidemia (%)	189 (43.4)	29 (46.8)	0.658
Diabetes mellitus (%)	121 (28.0)	33 (53.2)	0.001

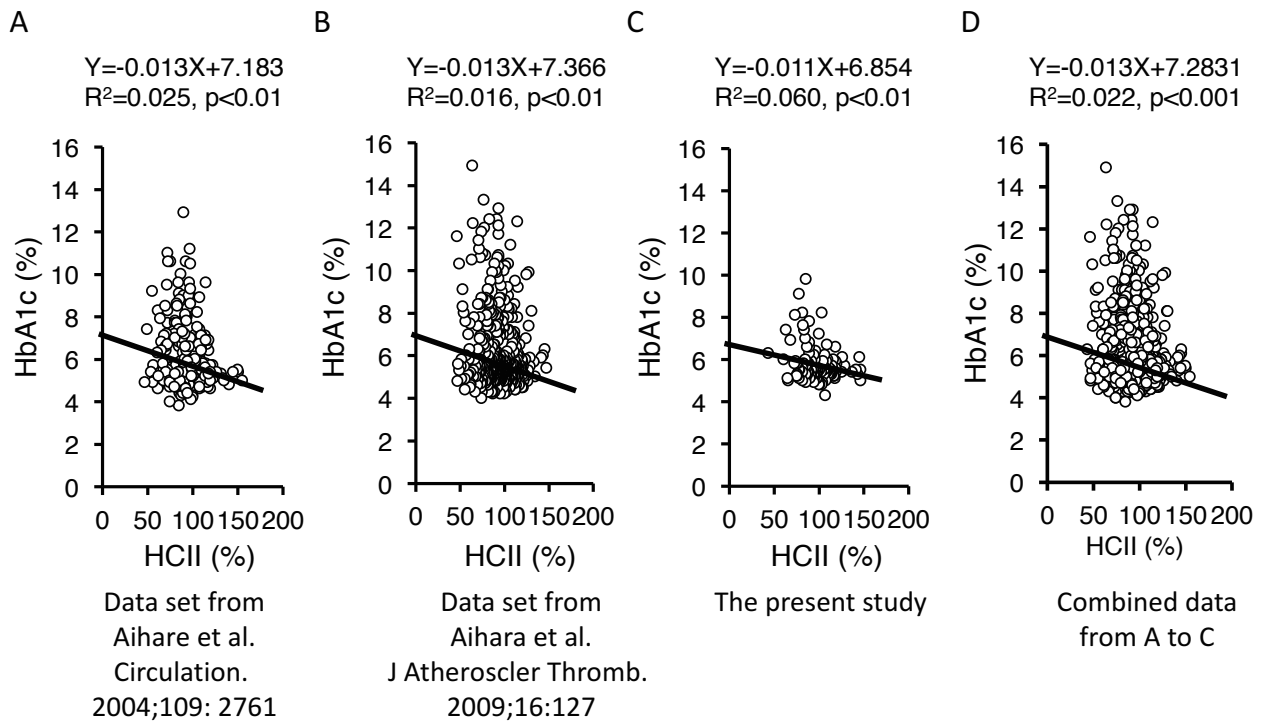Values are means ± SD or percentages.
Baseline characteristics were compared between ABI ≥ 0.9 and ABI < 0.9 by unpaired t test or χ^2 test for independence.
(Referred from the article by Aihara *et al*. J Atheroscler Thromb. 2009; 16: 127-134.)

Advance Publication
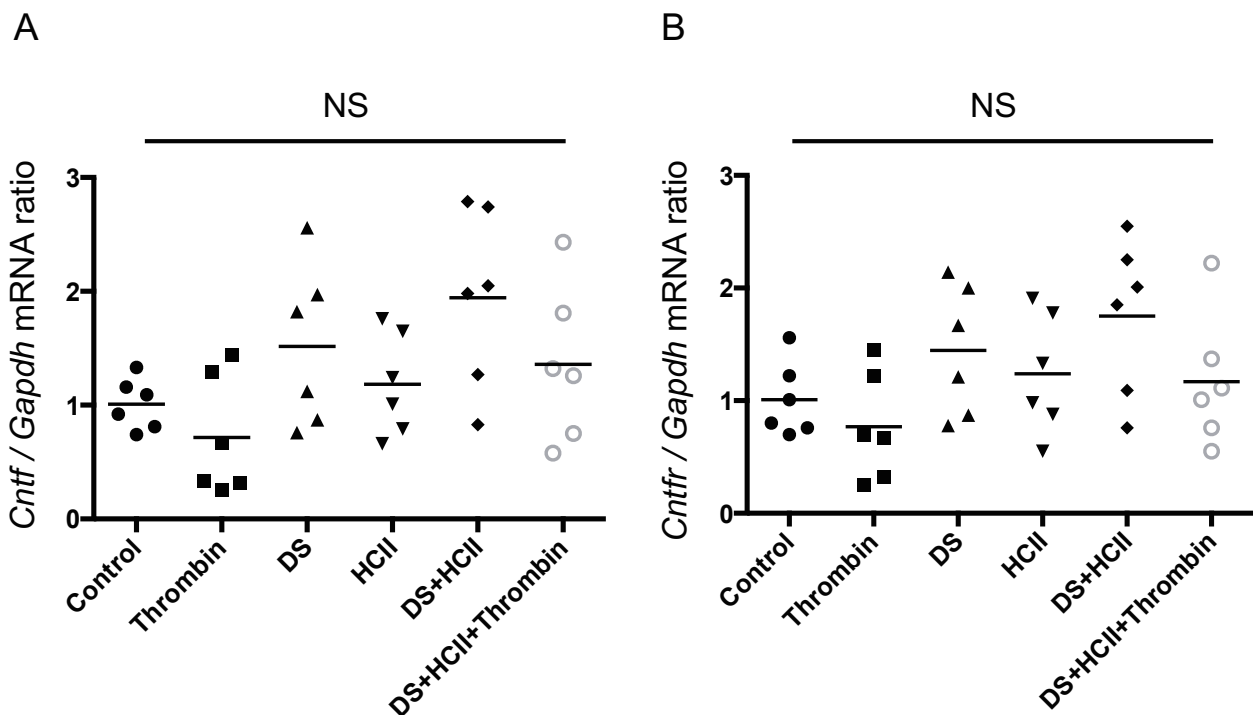Journal of Atherosclerosis and Thrombosis
Accepted for publication: March 28, 2017
Published online: May 15, 2017

Heparin Cofactor II and Hyperglycemia

Supplemental Table 3.

| Position | Symbol | Description | Fold Change (comparing to HCII-WT mice fed a HFD) | | |
| | | | HCII-deficient mice fed a HFD | | |
			Fold Change	95% CI	*p*-Value
A01	Adcyap1	Adenylate cyclase activating polypeptide 1	1.3553	(0.00001, 2.95)	0.517354
A02	Adcyap1r1	Adenylate cyclase activating polypeptide 1 receptor 1	0.6598	(0.30, 1.02)	0.248703
A03	Adipoq	Adiponectin, C1Q and collagen domain containing	0.7423	(0.48, 1.01)	0.101473
A04	Adipor1	Adiponectin receptor 1	0.8187	(0.67, 0.96)	0.046135
A05	Adipor2	Adiponectin receptor 2	0.7263	(0.37, 1.08)	0.237507
A06	Adra2b	Adrenergic receptor, alpha 2b	1.005	(0.42, 1.59)	0.926584
A07	Adrb1	Adrenergic receptor, beta 1	1.0728	(0.23, 1.91)	0.752198
A08	Agrp	Agouti related protein	0.7386	(0.53, 0.95)	0.071847
A09	Apoa4	Apolipoprotein A-IV	0.8082	(0.55, 1.06)	0.207946
A10	Atrn	Attractin	0.7263	(0.55, 0.90)	0.036849
A11	Bdnf	Brain derived neurotrophic factor	1.3117	(0.75, 1.87)	0.178754
A12	Brs3	Bombesin-like receptor 3	0.8082	(0.55, 1.06)	0.207946
B01	C3	Complement component 3	1.2533	(0.86, 1.65)	0.166931
B02	Calca	Calcitonin/calcitonin-related polypeptide, alpha	0.7306	(0.36, 1.10)	0.234034
B03	Calcr	Calcitonin receptor	1.3796	(0.00001, 3.05)	0.518477
B04	Cartpt	CART prepropeptide	0.6637	(0.41, 0.92)	0.07998
B05	Cck	Cholecystokinin	3.1821	(0.00001, 9.22)	0.275644
B06	Cckar	Cholecystokinin A receptor	1.9166	(0.00001, 4.61)	0.35273
B07	Clps	Colipase, pancreatic	1.417	(0.03, 2.80)	0.895452
B08	Cnr1	Cannabinoid receptor 1 (brain)	0.9184	(0.56, 1.27)	0.77961
B09	Cntfr	Ciliary neurotrophic factor receptor	0.4749	(0.29, 0.66)	0.005242
B10	Cpd	Carboxypeptidase D	1.0539	(0.76, 1.35)	0.666465
B11	Cpe	Carboxypeptidase E	1.0792	(0.56, 1.60)	0.6268
B12	Crhr1	Corticotropin releasing hormone receptor 1	1.2311	(0.00, 2.46)	0.508164
C01	Drd1a	Dopamine receptor D1A	0.4642	(0.12, 0.81)	0.1923
C02	Drd2	Dopamine receptor D2	0.6443	(0.42, 0.87)	0.043683
C03	Gal	Galanin	0.8442	(0.23, 1.46)	0.930742
C04	Galr1	Galanin receptor 1	1.434	(0.35, 2.52)	0.323728
C05	Gcg	Glucagon	0.7156	(0.50, 0.94)	0.065372
C06	Gcgr	Glucagon receptor	0.6864	(0.00001, 1.88)	0.15625
C07	Gh	Growth hormone	1.0612	(0.39, 1.73)	0.578551
C08	Ghr	Growth hormone receptor	0.8019	(0.52, 1.08)	0.199447
C09	Ghrl	Ghrelin	0.5401	(0.21, 0.87)	0.133176
C10	Ghsr	Growth hormone secretagogue receptor	1.3499	(0.00001, 3.00)	0.455813
C11	Glp1r	Glucagon-like peptide 1 receptor	0.7071	(0.39, 1.03)	0.157053
C12	Mchr1	Melanin-concentrating hormone receptor 1	1.3553	(0.00001, 2.95)	0.705335
D01	Grp	Gastrin releasing peptide	1.3526	(0.00001, 2.74)	0.919938
D02	Grpr	Gastrin releasing peptide receptor	0.903	(0.38, 1.43)	0.278168
D03	Hcrt	Hypocretin	1.2483	(0.00001, 2.53)	0.509901
D04	Hcrtr1	Hypocretin (orexin) receptor 1	0.5946	(0.34, 0.85)	0.051138
D05	Hrh1	Histamine receptor H1	1.6213	(0.56, 2.68)	0.239564
D06	Htr2c	5-hydroxytryptamine (serotonin) receptor 2C	1.005	(0.37, 1.64)	0.449317
D07	Iapp	Islet amyloid polypeptide	0.9238	(0.47, 1.37)	0.388305
D08	Il1a	Interleukin 1 alpha	0.6837	(0.06, 1.31)	0.257391
D09	Il1b	Interleukin 1 beta	1.879	(0.96, 2.80)	0.065358
D10	Il1r1	Interleukin 1 receptor, type I	0.8671	(0.61, 1.13)	0.298529
D11	Il6	Interleukin 6	1.3906	(0.22, 2.56)	0.233615
D12	Il6ra	Interleukin 6 receptor, alpha	1.022	(0.68, 1.37)	0.944864

(Cont Supplemental Table 3)

Position	Symbol	Description	Fold Change (comparing to HCII-WT mice fed a HFD)		
			HCII-deficient mice fed a HFD		
			Fold Change	95% CI	*p*-Value
E01	Ins1	Insulin I	1.3486	(0.00001, 2.93)	0.517016
E02	Ins2	Insulin II	0.7571	(0.54, 0.98)	0.109651
E03	Insr	Insulin receptor	0.6552	(0.36, 0.95)	0.119759
E04	Lep	Leptin	1.2422	(0.50, 1.99)	0.223664
E05	Lepr	Leptin receptor	0.9284	(0.45, 1.41)	0.979422
E06	Mc3r	Melanocortin 3 receptor	0.9257	(0.47, 1.38)	0.390157
E07	Nmb	Neuromedin B	0.6029	(0.26, 0.95)	0.263443
E08	Nmbr	Neuromedin B receptor	0.5223	(0.07, 0.97)	0.293177
E09	Nmu	Neuromedin U	0.5917	(0.30, 0.88)	0.126651
E10	Nmur1	Neuromedin U receptor 1	0.6235	(0.00001, 1.34)	0.297705
E11	Npy	Neuropeptide Y	1.6439	(0.00001, 3.61)	0.820424
E12	Npy1r	Neuropeptide Y receptor Y1	0.8459	(0.47, 1.22)	0.369206
F01	Nr3c1	Nuclear receptor subfamily 3, group C, member 1	0.7198	(0.57, 0.87)	0.008339
F02	Ntrk2	Neurotrophic tyrosine kinase, receptor, type 2	0.9004	(0.62, 1.19)	0.576791
F03	Nts	Neurotensin	1.4875	(0.00001, 3.75)	0.900008
F04	Ntsr1	Neurotensin receptor 1	1.1476	(0.49, 1.80)	0.700402
F05	Oprk1	Opioid receptor, kappa 1	0.8476	(0.54, 1.16)	0.283696
F06	Oprm1	Opioid receptor, mu 1	0.7586	(0.47, 1.05)	0.140887
F07	Sigmar1	Sigma non-opioid intracellular receptor 1	0.7738	(0.61, 0.94)	0.034028
F08	Pomc	Pro-opiomelanocortin-alpha	0.6988	(0.51, 0.89)	0.025299
F09	Ppara	Peroxisome proliferator activated receptor alpha	0.5285	(0.16, 0.90)	0.042418
F10	Pparg	Peroxisome proliferator activated receptor gamma	0.6199	(0.35, 0.89)	0.078419
F11	Ppargc1a	Peroxisome proliferative activated receptor, gamma, coactivator 1 alpha	0.3884	(0.19, 0.59)	0.014167
F12	Prlhr	Prolactin releasing hormone receptor	0.9367	(0.46, 1.41)	0.400798
G01	Ptpn1	Protein tyrosine phosphatase, non-receptor type 1	0.7908	(0.65, 0.93)	0.026759
G02	Pyy	Peptide YY	0.7489	(0.34, 1.16)	0.173387
G03	Ramp3	Receptor (calcitonin) activity modifying protein 3	1.188	(0.00001, 2.47)	0.620546
G04	Sort1	Sortilin 1	0.6481	(0.43, 0.87)	0.025804
G05	Sst	Somatostatin	0.7177	(0.50, 0.94)	0.066392
G06	Sstr2	Somatostatin receptor 2	0.732	(0.02, 1.44)	0.364054
G07	Thrb	Thyroid hormone receptor beta	0.9442	(0.67, 1.22)	0.856009
G08	Tnf	Tumor necrosis factor	1.2758	(0.07, 2.49)	0.671972
G09	Trh	Thyrotropin releasing hormone	0.77	(0.36, 1.18)	0.493715
G10	Ucn	Urocortin	0.6571	(0.41, 0.91)	0.080877
G11	Ucp1	Uncoupling protein 1 (mitochondrial, proton carrier)	0.9574	(0.57, 1.35)	0.920895
G12	Zfp91	Zinc finger protein 91	0.856	(0.68, 1.03)	0.174067
H01	Gusb	Glucuronidase, beta	1.001	(0.64, 1.36)	0.781711
H02	Hprt	Hypoxanthine guanine phosphoribosyl transferase	0.8501	(0.70, 1.00)	0.110094
H03	Hsp90ab1	Heat shock protein 90 alpha (cytosolic), class B member 1	1.1052	(0.84, 1.37)	0.398062
H04	Gapdh	Glyceraldehyde-3-phosphate dehydrogenase	0.8409	(0.65, 1.03)	0.147432
H05	Actb	Actin, beta	1.2645	(0.90, 1.63)	0.138857
H06	MGDC	Mouse Genomic DNA Contamination	1.1151	(0.21, 2.02)	0.489386
H07	RTC	Reverse Transcription Control	1.2311	(0.00, 2.46)	0.508164
H08	RTC	Reverse Transcription Control	1.1544	(0.14, 2.17)	0.497475
H09	RTC	Reverse Transcription Control	0.8228	(0.55, 1.10)	0.237255
H10	PPC	Positive PCR Control	0.9423	(0.46, 1.43)	0.405995
H11	PPC	Positive PCR Control	0.9564	(0.48, 1.43)	0.469732
H12	PPC	Positive PCR Control	0.9564	(0.44, 1.47)	0.4568

14

Heparin Cofactor Ⅱ and Hyperglycemia

A

Y=-0.013X+7.183
R²=0.025, p<0.01

HbA1c (%)

HCII (%)

Data set from
Aihare et al.
Circulation.
2004;109: 2761

B

Y=-0.013X+7.366
R²=0.016, p<0.01

HbA1c (%)

HCII (%)

Data set from
Aihara et al.
J Atheroscler Thromb.
2009;16:127

C

Y=-0.011X+6.854
R²=0.060, p<0.01

HbA1c (%)

HCII (%)

The present study

D

Y=-0.013X+7.2831
R²=0.022, p<0.001

HbA1c (%)

HCII (%)

Combined data
from A to C

Supplemental Fig. 1. Scatter plots of plasma HCⅡ activity and HbA1c values in our previous studies (A: $n = 130$ and B: $n = 494$), the present study (C: $n = 130$), and all studies combined (D: $n = 930$)

A

NS

Cntf / Gapdh mRNA ratio

Control Thrombin DS HCII DS+HCII DS+HCII+Thrombin

B

NS

Cntfr / Gapdh mRNA ratio

Control Thrombin DS HCII DS+HCII DS+HCII+Thrombin

Supplemental Fig. 2. The 3T3-L1 preadipocytes were cultured as previously described (Mihara M *et al.* Endocrinology. 2010; 151: 513-519.) and the cells plated onto six-well dishes were treated with thrombin (1 U/ml) or human purified heparin cofactor Ⅱ (HCⅡ) (100 nM) or dermatan sulfate (DS) (5 μg/ml) for 48 h. $n = 6$ in each group. NS means not significant.

Kurahashi *et al.*

A

B
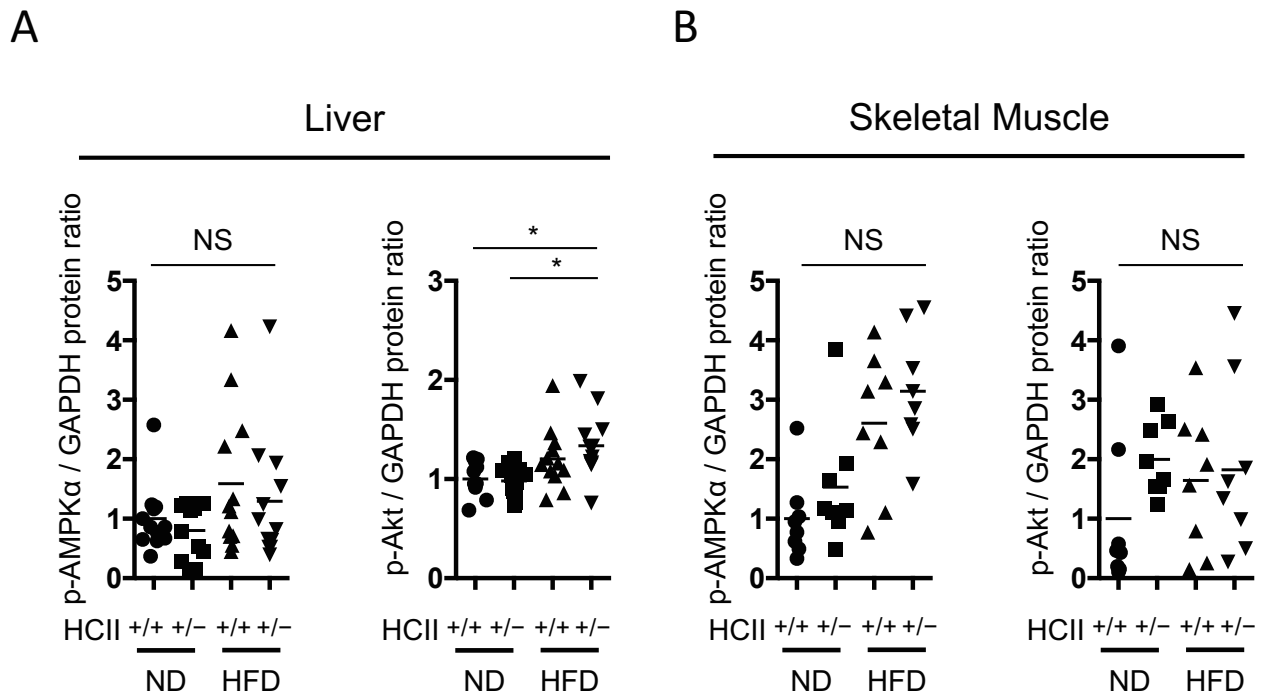
Supplemental Fig. 3. Quantitative results of phosphorylated AMPK-to-GAPDH protein ratios and phosphorylated Akt-to-GAPDH protein ratios in hepatic tissues and skeletal muscle (thigh) of $HCII^{+/+}$ mice and $HCII^{+/-}$ mice with ND or HFD feeding, $n = 8$ to 12 in each group. Bars represent mean values in each group. $^{*}p < 0.05$, NS means not significant.